JOURNAL OF PROPULSION AND POWER
Vol. 18, No. 6, November–December 2002

Proportional Control of Combustion Instabilities in a Simulated Gas-Turbine Combustor

Christian Oliver Paschereit*
Alstom (Switzerland) Ltd., 5405 Baden, Switzerland
and
Ephraim Gutmark†
University of Cincinnati, Cincinnati, Ohio 45221

Unstable thermoacoustic modes were investigated and controlled in an experimental low-emission swirl-stabilized combustor. Axisymmetric and helical unstable modes were identified for fully premixed combustion. The spatial location of intense combustion regions associated with the different unstable modes was visualized by phase-locked images of OH chemiluminescence. The axisymmetric mode showed large variation of the heat release during one cycle, whereas the helical modes showed circumferential variations in the location of maximal heat release. An acoustic closed-loop proportional active control system was employed to suppress the thermoacoustic pressure oscillations and to reduce NO_x emissions. Microphone sensors were utilized to monitor the combustion process and provide input to the control system. Acoustic actuation was utilized to modulate the airflow and affect the mixing process and the combustion processes. Equivalence ratio modulations were not employed in the present controller. Suppression in the pressure oscillation levels of over 12 dB, and a concomitant 10% reduction of NO_x emissions were achieved using an acoustic power of less than 0.002% of the combustion power. The proportional controller was superior to a phase lag controller that yielded a maximum suppression of 4 dB at the same level of acoustic power. At the optimal control conditions it was shown that the major effect of the control system was to reduce the coherence of the vortical structures, which gave rise to the thermoacoustic instability.

Introduction

LARGE-SCALE coherent structures play an important role in combustion and heat-release processes by controlling the mixing between fuel and air in diffusion flame configurations and the mixing between the fresh fuel/air mixture and hot combustion products and fresh air in premixed combustors. The evolution of these structures in nonreacting flows was extensively studied in mixing layers,[1,2] jets,[3,4] and flows over backward-facing steps.[5] However, studies of large structures in swirling flows are scarce. Unlike large-scale structures in nonswirling flows, which are predominantly axisymmetric, swirl enhances azimuthal unstable modes. Interaction between large-scale structures that are related to flow instabilities, acoustic resonant modes in the combustion chamber, and the heat-release process has been shown to cause undesired thermoacoustic instabilities in combustors.[6] The effect of swirl on the longitudinal and azimuthal instability modes and the way it modifies the combustion process leading to thermoacoustic instabilities requires further investigation.

Realizing the importance of large-scale structures as potential drivers of combustion instabilities, researchers developed passive and active methods to control instabilities by modifying the vortical structures in the flow.[7–9] Most of these control methods were applied to bluff-body-stabilized combustors and dump combustors in which the flow recirculation is used to stabilize the flame. Various passive and active control strategies have been used to suppress thermoacoustic instabilities resulting from coupling between the heat and pressure oscillations in these combustors (Rayleigh criterion[10]). One example for passive control strategy was to use noncircular geometries to enhance small-scale mixing, reduce the coherence of large-scale vortices, and generate axial vorticity. Another example for active control strategy was to utilize fuel modulations and phase shifting to decouple the pressure and heat-release cycles. Other control strategies have also investigated improving fuel efficiency and reducing pollutants[11] and extending flammability limits.[12]

Swirl stabilization is utilized in combustion systems such as gas turbines, which also exhibit combustion instabilities. Rational modification of large-scale vortices is important to control swirl-induced instability and reduce emissions. Control of swirling flows requires understanding of the vortical structure in this type of flow and the effect of forcing on the structure. Paschereit et al.[13–18] investigated instability modes in an experimental low-emission swirl-stabilized combustor and used acoustical control methods. Two operating modes were studied including a partially premixed and a premixed combustion. The partially premixed diffusion flame was tuned to unstable operation with two destabilized modes: axisymmetric and helical. The premixed instability mode, which was obtained by adjusting the acoustic boundary conditions, was predominantly axisymmetric. Pressure fluctuations were detected only for the axisymmetric modes, but heat-release fluctuations, which were measured by OH chemiluminescent emission,[19] indicated dual-mode behavior. A closed-loop active control system was employed to suppress combustion instabilities and to reduce emissions at various operating conditions.

The thermoacoustic instability control work was extended to include a more practical (compared to acoustic excitation) fuel modulation strategy.[20] Symmetric and antisymmetric fuel pulsations were used to control symmetric and helical instability modes. The modulated fuel injection was shown to effectively suppress pressure and heat-release oscillations and reduce emissions.

In the present work, instability modes in an experimental low-emission swirl-stabilized combustor were investigated and controlled using acoustic actuators. Unlike the previously used phase-lock/phase-shift (PLPS) controller, a proportional closed-loop active control system was employed to suppress combustion instabilities and to reduce emissions at various operating conditions.

Received 24 April 1999; revision received 15 September 2000; accepted for publication 26 June 2002.

*Manager of Basic Combustion Technologies, Im Segelhof 1; oliver.paschereit@power.alstom.com. Member AIAA.

†Ohio Eminent Scholar and Professor, Department of Aerospace Engineering and Engineering Mechanics; Ephraim.Gutmark@uc.edu. Associate Fellow AIAA.

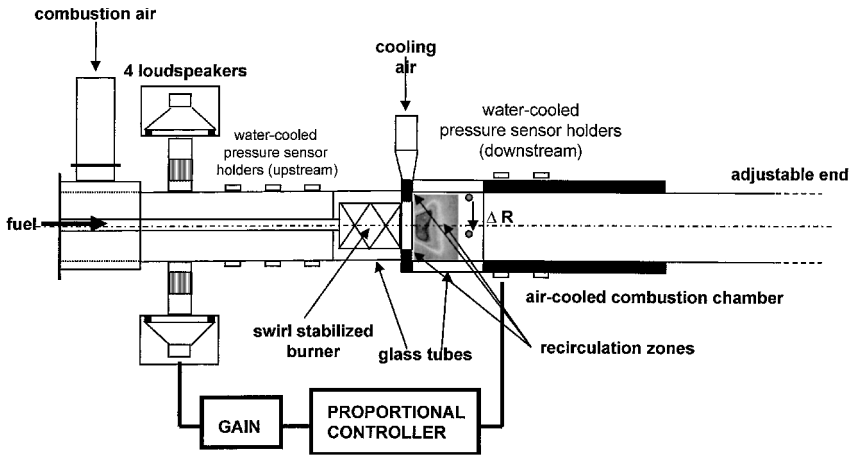

Fig. 1 Experimental arrangement of the combustor.

The controller utilized a digital signal-processing unit to feed back the original pressure pulsation signal after a predetermined phase shift to drive the loudspeakers. The effect of the control system on the structure of the unstable modes and combustor performance is reported.

Experimental Setup

Combustion Facility

The combustion facility is shown in Fig. 1. The atmospheric test rig consists of a plenum chamber upstream of the swirl-inducing burner and a combustion chamber downstream of the burner. The plenum chamber contains perforated plates to modify the turbulence level of the flow. The circular combustion chamber consists of air-cooled double-wall quartz glass to provide full visual access to the flame. The exhaust system is an air-cooled tube with the same cross-section as the combustion chamber to avoid acoustic reflections at area discontinuities. The acoustic boundary conditions of the exhaust system could be adjusted by placing in the exhaust tube orifice plates with various opening diameter, from almost anechoic (reflection coefficient $|r| < 0.15$) to open-end reflection. To determine the acoustic characteristics of the burner nozzle/flame, the up- and downstream propagating waves f and g (Riemann invariants) have to be determined.[15] Acoustic properties such as impedance $Z = p/u$ or the acoustic reflection coefficient $r = g/f$ can then be calculated from the measured Riemann invariants.

An experimental swirl-stabilized premixed burner was used in the experiments. Natural gas was injected into the swirling vanes to ensure homogeneous mixing of air and fuel. The burner was operated at a Reynolds number of $Re = 8 \times 10^4$, a swirl number of $S = 0.7$, and a combustor length to diameter ratio $L/D = 4.5$. The flame was stabilized in the recirculation regions near the burner outlet. As shown in Fig. 1, the flowfield produced by the swirling flow resembled an annular jet with a central recirculating region and a circumferential recirculation region behind the backward-facing step.[14] Controlled excitation of the burner flow was accomplished by a circumferential array of four loudspeakers equally spaced in polar angle and located upstream from the burner at a distance of $x = 2.4D$ upstream of the dump plane. The acoustic power used to achieve control was less than 0.002% of the combustion power. For axisymmetric disturbances the loudspeakers were operated at zero phase difference. Pressure fluctuations were measured using Brüel and Kjær water-cooled $\frac{1}{4}$-in. condenser microphones with frequency range of up to 100 kHz. Time varying heat-release was recorded with two bandpass-filtered fiber-optic probes with a lower and higher cut-off wavelength of 290 and 390 nm to detect OH radiation. The emission spectrum within this window includes also intermediate species such as NO, NH, and CN, but at a level that is about an order of magnitude lower.[21] The circular field of view of the probes had a diameter of 10 mm at the flame position. The probe was coupled with a photomultiplier yielding a maximum frequency response of 10.7 kHz.

Control and Visualization Systems

A schematic diagram of the closed-loop control system is given in Fig. 1. Pressure sensors microphones were utilized to monitor the combustion process and provide input to the control system. The signal of the microphone was digitally delayed and amplified before being fed back to drive the loudspeakers through an audio amplifier. This proportional controller was different than previously employed PLPS controller in which the narrowband-filtered microphone signal was used as a trigger to produce a sine wave at the dominant frequency and at a predetermined phase delay relative to the trigger signal, to drive the loudspeakers. Acoustic actuation was utilized to modulate the airflow entering the swirl-generating burner. Phase-locked pictures of the flame were obtained using an amplified (microchannel plate) Charge-Coupled Device (CCD) camera with an exposure time of 20 μs. The camera was triggered by the pressure signals that were bandpass-filtered at the instability frequency and phase shifted. The images were filtered using a bandpass filter with low and high cutoff wavelengths of 290 and 390 nm, respectively, to visualize OH concentration. The phase-locked exposures were then averaged over 64 events, representing the coherent features of the flame structure. The operating conditions of the burner have been maintained by analyzing the exhaust gas composition using a physical gas analysis system. CO and CO_2 have been analyzed by using nondispersive infrared spectroscopy. The nitric oxides NO and NO_2, combined in NO_x, have been detected with a chemiluminescence analyzer. The measured emissions were corrected to 15% oxygen basis. The detection of the remaining O_2 in the exhaust gas was made utilizing the paramagnetic properties of oxygen in the analyzing device.

Results and Discussion

Structure of Combustion Instabilities

Naturally occuring low-level axisymmetric and helical thermoacoustic instability modes were amplified by adjusting the acoustic boundary conditions of the combustor for various power outputs and equivalence ratios. The instability modes, in the present experiment, were related to combustion within large-scale structures, which were excited in the combustion chamber as a result of interaction between flow instabilities and the acoustic resonant modes of the combustor as determined by the combustion chamber acoustic boundary conditions.[13] Additional source of instabilities, which can be dominant in combustion processes, are equivalence ratio modulations.[22] The instabilities associated with the premixed mode of operation were at normalized frequencies $St = fD/\bar{U} = 0.58$ and at $St = 1.16$, where f is the instability frequency, D the burner diameter, and $\bar{U}$ the burner's average exit velocity. The different instability modes were visualized using an amplified and filtered CCD camera that was triggered at different phase angles relative to the instability pressure signal. Using this technique, phase-averaged OH images were obtained for different thermoacoustic instabilities. In a previous publication[16] the flame structure was visualized in the

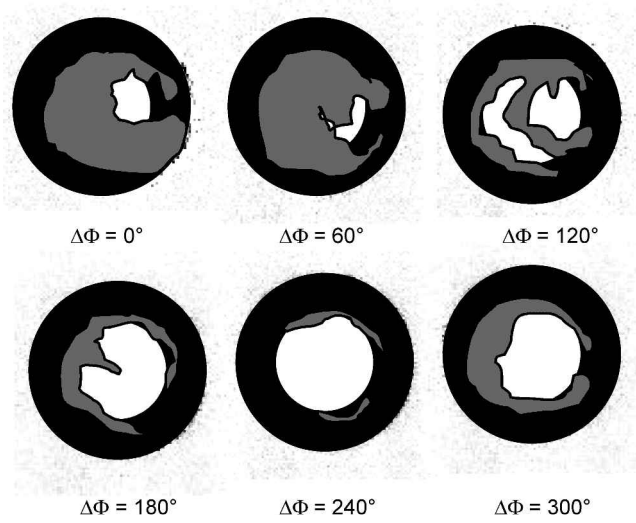

Fig. 2 Phase-averaged visualization of the low-frequency axisymmetric instability ($St = 0.58$) during one instability cycle. Cross-hatched area indicates flame zone.

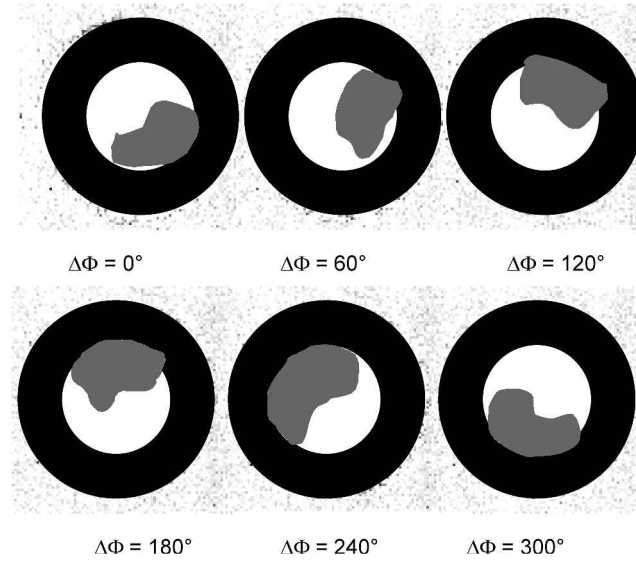

Fig. 3 Phase-averaged visualization of the low-frequency helical instability ($St = 1.16$) during one instability cycle. Cross-hatched area indicates flame zone.

x–r plane, exhibiting the longitudinal and radial variation during a cycle of instability. For the axisymmetric unstable mode OH chemiluminescence showed variation of the heat release during a cycle of instability, while maintaining axisymmetric structure. In the helical mode the total heat release did not vary during a cycle, but the location of heat release varied circumferentially. The spatial integration of heat release did not vary during a cycle, and as predicted for such case by the Rayleigh criterion the corresponding acoustic mode was not excited.

The flame was visualized from the back end of the combustor yielding an integrated cross-sectional cut. The axisymmetric $St = 0.58$ instability is shown in Fig. 2 at phase angles between 0 and 300 deg every 60 deg, for a normalized air excess ratio of $\lambda/\lambda_n = 1$, in premixed operation. λ_n is the nominal inverse equivalence ratio ($\lambda_n = 1/\phi_n$, where ϕ_n is the nominal equivalence ratio), which is the optimal lean premixed operating condition of the combustor. The images were filtered using a bandpass filter at 290 nm $< \lambda <$ 390 nm and show the OH emission of the flame indicating the combustion zones. The variable heat release during the cycle is evident from the images. The lowest heat release, indicated by low value of OH intensity, was measured at phase angles of 240–300 deg, whereas the highest level was measured at 60–120 deg. In addition to the axisymmetric mode, a helical unstable mode was measured at a higher frequency ($St = 1.16$) at an air excess ratio of $\lambda/\lambda_n = 1.1$ (Fig. 3). The images are similar to those shown in Fig. 2. Areas of high concentration of OH were outlined for clarity. The high OH intensity moved circumferentially, completing one instability cycle, as shown by the images that are presented at the different phase angles. These observations confirm the earlier conclusions regarding the different nature of the axisymmetric and helical unstable modes, that is, axisymmetric heat-release temporal variation during an instability cycle vs circumferential spatial variation of heat release for helical instability mode.

Combustion Control

Pressure and OH Oscillations

A closed-loop proportional feedback control system was designed to reduce the coherence of the large-scale structures thus to suppress the level of pressure oscillations caused by combustion instability. Speakers were installed at the upstream end of the experimental setup at a distance of $x = 2.4D$ upstream of the dump plane, providing excitation of the central and circumferential shear layers of the annular jet exiting the burner (Fig. 1). The control system was based on a microphone that monitored pressure fluctuations in the combustor as a result of the acoustic resonance of the chamber. The feedback loop consisted of a digital signal processing unit that fed the original microphone signal back to the speakers after a predetermined delay and amplification. The phase shift between the microphone signal and the speakers driving signal was varied over a full instability cycle. The effect on the pressure fluctuations amplitude at the instability frequency was recorded. The level of OH fluctuations in the shear layer at an axial distance of $x/D = 0.5$ was simultaneously recorded. The variation of the pressure and OH oscillations as a function of the relative phase between the microphone (sensor) and speakers (actuators) is shown in Fig. 4 for the axisymmetric unstable mode at $St = 0.58$. The controlled behavior is compared with the straight horizontal line that depicts the baseline pressure and OH fluctuations levels when the controller is not operating. Maximum suppression was obtained at a phase difference of 60 deg, whereas maximum destabilization of the combustion was observed at 270 deg. At the optimal phase angle the instability was suppressed by over 12 dB, and the maximum amplification was 1.4 dB. This large difference between the suppression and amplification levels is an indication of the high degree of coherence of the uncontrolled combustion structures, whose regularity could not be enhanced to a higher level by in-phase forcing. The high suppression level is a significant improvement relative to previous results of 4.2 dB suppression obtained with a PLPS controller as shown in the figure for comparison. The optimal phase shift of the PLPS controller was different than that of the proportional controller because of the difference in the convective time delays and phase shifts that were introduced by the control circuits in the two systems. Figure 5 shows a comparison between the uncontrolled pressure spectrum and the spectra of the reduced level pressure oscillations for the PLPS and proportional controllers for operation at the corresponding optimal phase shift with pressure monitoring. The PLPS controller produced

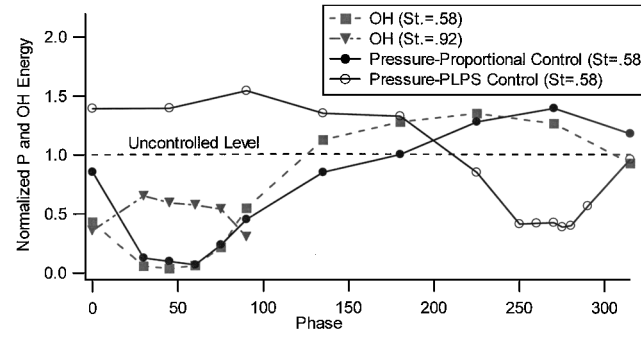

Fig. 4 Normalized energy of the pressure and OH oscillations for various control phase angles.

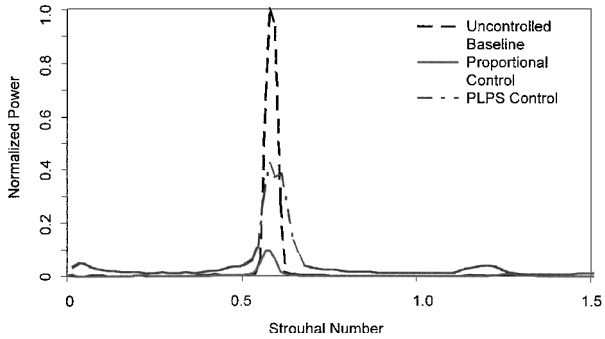

Fig. 5 Normalized power spectra of the pressure oscillations at the instability frequency comparing no control with PLPS and proportional control.

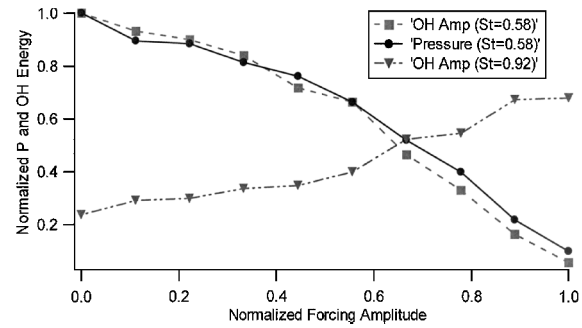

Fig. 6 Energy of the pressure and OH fluctuations as a function of forcing amplitude.

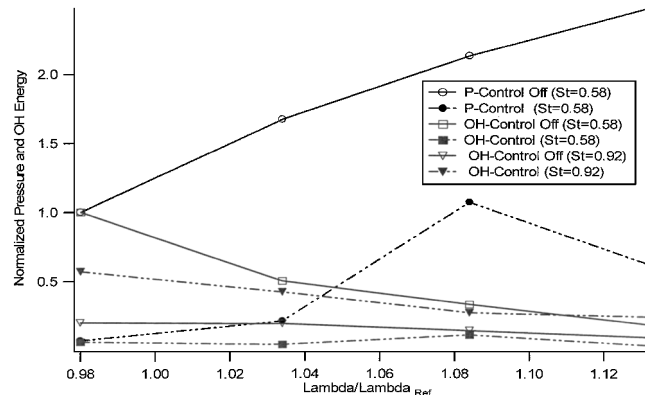

Fig. 7 Amplitude of the pressure and OH fluctuations as a function of air excess ratio.

a sinusoidal signal to drive the speaker at a predetermined phase angle relative to the microphone signal.[16] In that case the driving signal was at a single frequency, matching the average instability frequency. The PLPS controller achieved a maximum suppression of less than 4 dB at the same conditions. Amplification level at the off-design conditions was similar to the present results. The advantage of the present controller over the PLPS controller is in the fact that the input signal is based on the instability signal itself. Thus, the spectral energy distribution as well as the phase information represents the physical behavior of the system at all times. The PLPS controller uses an artificially generated signal at a fixed frequency, which represents the average, most energetic mode but whose frequency content, amplitude, and phase are not following accurately the real variations of the instability signal as conditions in the combustor vary. The proportional controller can follow continuously a broad variable instability and react to small changes in frequency and phase, so that the control signal can be modified accordingly. A control signal that is synthesized based on time-averaged frequency will intermittently be the correct signal. Also, as the amplitude of the instability is reduced by the controller the control signal is reduced proportionally and does not cause further destabilization by continuing to drive the actuator at a large amplitude even after suppression is achieved, as the PLPS controller does.

The variation of the OH oscillations for the different phase angles of microphone-based control were measured and shown in Fig. 4. These measurements are indicative of the effect of the control system on the flow structure. The maximal suppression of the OH oscillations was obtained in the range of 30–60 deg. The OH fluctuations were reduced by over 12 dB indicating that the large-scale structures had lost their coherence. This reduction in coherence is also supported by evidence shown later in Figs. 10 and 11. For comparison, the PLPS controller yielded 3-dB reduction in OH fluctuations at the optimal phase. At the range of 0–100 deg, which yielded the largest suppression of OH fluctuations, secondary heat-release oscillations at $St = 0.92$ were observed. However, their maximum level never exceeded 60% of the original level of the $St = 0.58$ instability, and pressure oscillations were not excited at this frequency because it did not couple with any acoustic mode in the combustor. The appearance of the secondary heat-release fluctuations was a result of amplification of secondary natural modes in the flow at frequencies, which are destabilized by the same phase that stabilized the main instability because the optimal suppression phase changes with frequency. The amplitude of OH fluctuations was increased at 180 deg off the optimal phase angle, indicating enhancement of the combustion in the large-scale coherent structures.

The amplification (gain setting) of the control signal was varied to study its effect on the reduction of pressure and OH oscillations at the optimal phase of 50 deg. The results in Fig. 6 show that the energy of both the pressure and OH fluctuations decreased proportionally to the gain, reaching a negligible level at maximum gain. The figure also shows the destabilization of a secondary heat release mode at $St = 0.92$ with increased gain without exciting the pressure pulsations at this frequency.

The efficiency of the control system was determined in a range of combustor equivalence ratios, using the optimal phase of 50 deg and a maximum gain level (Fig. 7). The equivalence ratio was varied by changing the fuel mass flow rate while maintaining the airflow rate constant. The optimal phase did not vary with equivalence ratio but did vary with power as discussed later. Reduction in pressure and OH oscillations were observed in an air excess ratio range of $0.98 < \lambda/\lambda_n < 1.17$. The level of the uncontrolled pressure oscillations increased for leaner fuel/air mixtures. The level of the controlled pressure oscillations was also dependent on the fuel-to-air ratio so that the relative suppression levels remained unchanged as the lean blowout limit was approached at a normalized air-to-fuel ratio of 1.125. The uncontrolled OH fluctuations were strongly dependent on the fuel-to-air ratio. As the mixture became leaner, their level was reduced as a result of a shift in the combustion zone relative to the stationary OH probe. The controlled OH fluctuations were independent of the air excess ratio; thus, the apparent reduction level decreased at higher λ ratio. Simultaneously, the instability at $St = 0.92$ increased to a slightly higher degree at the low λ compared to a small effect at the high λ (Fig. 7).

The proportional controller was also evaluated at a combustor output power increase of 10% relative to Fig. 4, associated with an increase of the mass flow rate through the combustor. The variation of the pressure and OH oscillations as a function of the relative phase is shown in Fig. 8 for the axisymmetric unstable mode at $St = 0.58$. The range of phase shift for which suppression was obtained changed slightly relative to the lower power case as a result of the change in the flow velocity. Maximum suppression was obtained at a phase difference of 20 deg, whereas maximum destabilization of the combustion was observed at 240 deg. The gain used in the tests was the same as for the low power tests. At the optimal phase angle the pressure instability was suppressed by over 10 dB, and the maximum amplification was 0.5 dB. The OH fluctuations were reduced by nearly 10 dB indicating that the large-scale structures lost their coherence. Very slight increase in OH fluctuations was measured at off-design conditions. At a range of 30–60 deg, which yielded the largest suppression of OH fluctuations, the secondary instability at $St = 0.92$ was excited. In this case its level exceeded that

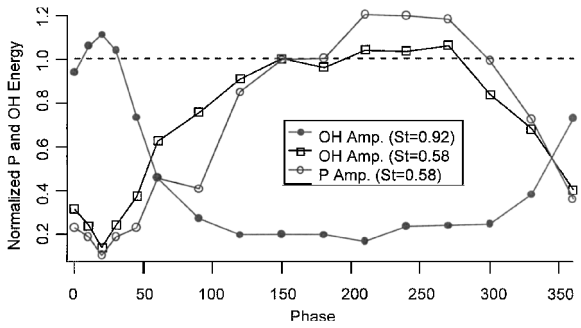

Fig. 8 Normalized energy of the pressure and OH oscillations for various control phase angles.

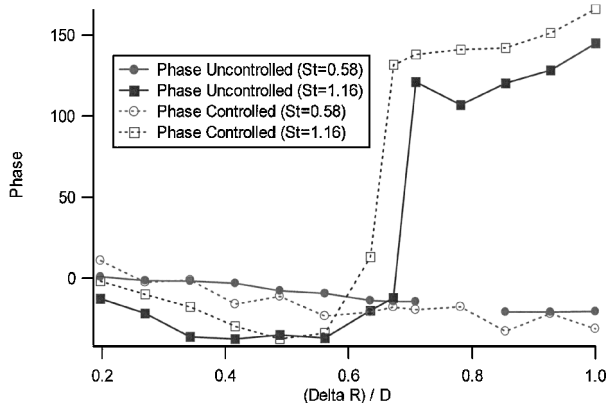

Fig. 9 Relative phase of radial OH cross correlations, without and with control.

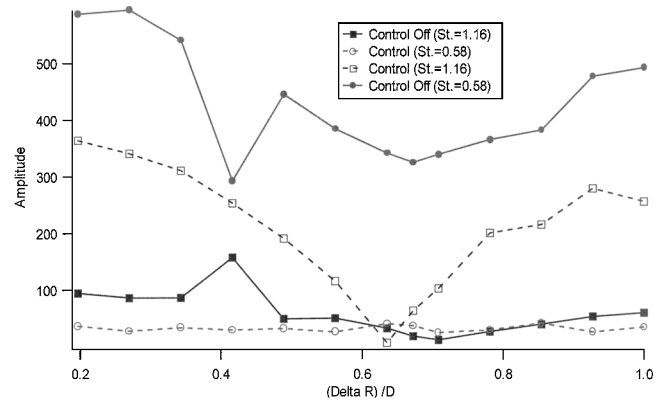

Fig. 10 Amplitude of radial OH cross correlations, without and with control.

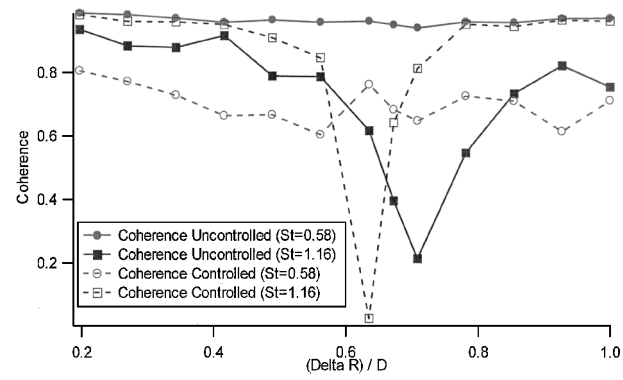

Fig. 11 Coherence of radial OH cross correlations, without and with control.

of the original level of the $St = 0.58$ instability in a narrow phase band between 10 and 30 deg. However, the pressure fluctuations at $St = 0.92$ were small in the entire range of phase angles.

Effect of Control on Combustion Structure

The structure of the reacting vortices inside the combustor was assessed from radial cross-correlation measurement between two filtered OH chemiluminescence fiber-optic probes. For the radial cross-correlation measurements one of the OH sensors was stationary in the upper shear-layer at an axial distance $x/D = 0.5$ from the dump plane, while the other one was traversing the combustion zone radially at the same axial distance. The axial distance of one-half burner diameter was chosen because it allowed high signal-to-noise ratio of the OH fluctuations in the middle of the reacting vortical flame zone.[13] The second probe was moving radially starting from the stationary probe ($\Delta R/D = 0$) until it reached the opposite shear-layer. The measurements were performed for two unstable Strouhal numbers, $St = 0.58$ (axisymmetric instability) and $St = 1.16$ (helical instability). The coherence function, the amplitude of the radial cross correlation, and the relative phase were measured at increased spacing ΔR between the two probes. The coherence function defined as the cross-spectral density of two signals of interest normalized by the individual power spectral densities. It gives a quantitative measure of the strength of the correlation between the two signals. In the present case, high coherence indicates the presence of a coherent vortical structure in the reaction zone. The relative phase angle between the two OH signals is plotted as a function of $\Delta R/D$ in Fig. 9. The self-excited instabilities at $St = 1.16$ underwent a phase change of nearly 180 deg corresponding to helical modes, whereas the mode at $St = 0.58$ remained close to zero phase angle across the combustor, indicative of an axisymmetric mode. Control did not change the phase behavior of the axisymmetric mode but shifted the helical mode phase change closer to 180 deg, corresponding to the strengthening of this mode.

The variation of the radial cross-correlation amplitude and coherence (Figs. 10 and 11, respectively) reflected the effect of the pressure controller on the combustion structure. The amplitude of the low-frequency axisymmetric cross correlation was significantly lowered, and the coherence function was reduced from one to nearly 0.6. Both indicate the weakening of the axisymmetric flame structure by the controller. At the same time the helical structures at $St = 1.16$ showed increased amplitude and coherence. This behavior corresponds to the destabilization of the helical mode by the proportional controller. Because the variation in OH intensity of the helical structures is mostly concentrated in the circumferential shear-layer[13] and its level near the combustor center is very low, both the cross-correlation amplitude and coherence approach zero in the center. In spite of the strengthening of the helical heat-release mode, it did not couple with any acoustic modes and thus did not lead to high-amplitude combustion instability.

Effect on CO and NO_x Emissions

NO_x and CO emissions were monitored in the entire range of phase used for pressure oscillation control. The results, depicted in Figs. 12 and 13, show a 20% reduction of the NO_x and virtually no effect on CO levels at the same phase shift range that yielded pressure fluctuations stabilization. A maximum of nearly 10% increase in NO_x emissions was observed at a phase shift of 180 deg relative to the optimal phase value. The concomitant NO_x emissions reduction and pressure oscillations suppression are both related to the reduced coherence of the vortical structures. Thermoacoustic instability is associated with periodic heat release, which occurs within vortices producing high peak temperature.[8,23] Control at the optimal phase range between 0–60 deg decreases the vortical coherence and enhances the fine-scale mixing, thus inhibiting peaks of heat release as indicated by the minimum in OH radiation and reduced coherence at these phase angles.

During stable combustion, an increase in temperature results in an increase in NO_x and a decrease in CO formation and the opposite behavior when the temperature is decreased. Because both NO_x and CO emission levels depend exponentially on temperature,[24] in unstable lean premixed combustion, fluctuations in heat-release (and

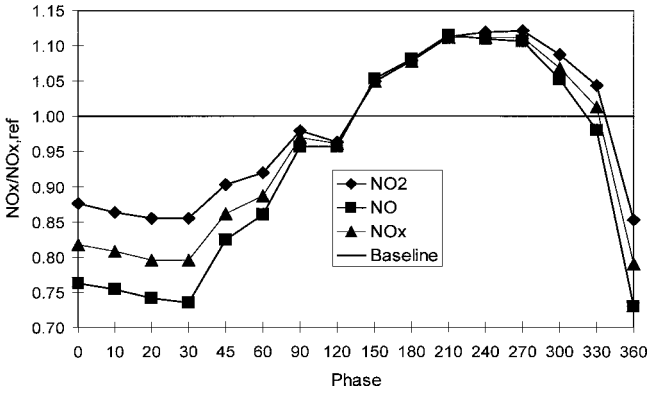

Fig. 12 NO_x emissions for various control phase angles.

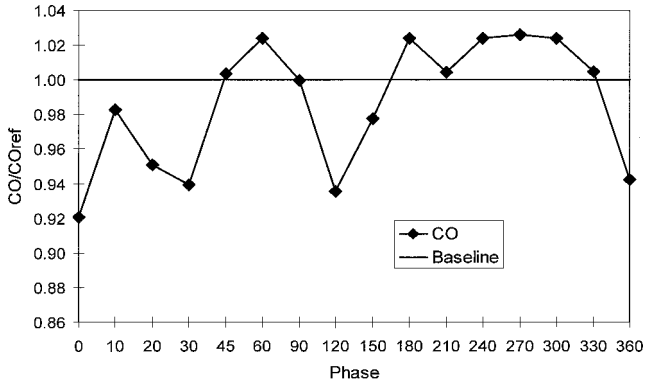

Fig. 13 CO emissions for various control phase angles.

consequently fluctuations in temperature) can lead to an increase in NO_x and CO; the exponential dependency of NO_x and CO formation on temperature causes the average emissions to be higher than the level at the operating point for steady-state conditions. By stabilizing the combustion process, it was therefore possible to obtain a concomitant decrease in NO_x with no significant effect on CO emission levels.

Conclusions

Proportional active combustion control using acoustic actuators was applied to an experimental low-emission swirl-stabilized combustor, in which the acoustic boundary conditions were modified to obtain unstable operation points. The acoustic actuators modified the flowfield and thus affected the mixing process. In addition, it caused modulations in the airstream, thus affecting the equivalence ratio with no concurrent effect on the fuel flow rate. Two unstable modes were investigated in fully premixed combustion: axisymmetric ($St = 0.58$) and helical ($St = 1.16$). The axisymmetric mode was excited at a Strouhal-number range within the observed most unstable mode (preferred mode) of a round jet.[3] The scaling of the instability frequency with the burner exit velocity would suggest linear variation of this frequency with temperature, whereas the acoustic frequency would vary with the square root of the temperature. This different dependency on temperature can explain the variation of the instability amplitude with power and equivalence ratio observed in this investigation. However, because of the broadband character of flow instabilities this detuning does not prevent the flow and acoustic modes from staying aligned provided that the changes in operating conditions are not excessive.

The combustion structure associated with the different unstable modes was visualized by phase-locked images of OH chemiluminescence. The axisymmetric mode showed large variation of heat release during a period of oscillation, while the helical modes showed azimuthal variations of maximal heat release.

A proportional closed-loop active control system was employed to suppress the thermoacoustic pressure oscillations while maintaining low NO_x and CO emissions. Suppression levels of over 12 dB in the pressure oscillations and a concomitant 20% reduction of NO_x without affecting CO emissions were obtained using a relatively low acoustic power of 0.002% of the combustion power in an air excess ratio range of $0.98 < \lambda/\lambda_n < 1.17$. The proportional controller was shown to have superior performance to that of the PLPS controller that yielded a maximum reduction of 4 dB at the same level of acoustic power. The improved performance is caused by the utilization of the time-shifted original signal to drive the actuator rather than a phase-shifted pure sine wave representing the major component of the instability. The advantage of the proportional controller over the PLPS controller is in the fact that the input signal is based on the instability signal itself. Thus, the spectral energy distribution as well as the phase information represents the physical behavior of the system at all time. In other words, the original signal contains spectral information that is necessary to achieve full suppression when the instability cannot be characterized solely by a single frequency. The PLPS controller uses an artificially generated signal at a fixed frequency, which represents the average most energetic mode but whose frequency distribution, amplitude, and phase are not following accurately the real signal as conditions of the combustion process vary. The proportional controller can thus follow continuously the variable instability and react to small variations in frequency and phase, modifying the control signal accordingly. Also, as the amplitude of the instability is reduced by the controller the control signal is reduced proportionally, and it does not cause further destabilization of the combustion by continuing to drive the actuator at a large amplitude even after suppression is achieved, as the PLPS controller does.

The optimal forcing level was determined by varying the gain of the time-delay unit increasing the amplitude of the actuator driving signal. The reduction of pressure oscillations was directly proportional to the forcing level in the range of parameters studied.

At the optimal control conditions it was shown that the major effect of the control system was to reduce the coherence of the vortical structures that gave rise to the axisymmetric thermoacoustic instability. OH chemiluminescence measurements showed that while the axisymmetric structures were suppressed a higher-frequency helical instability was amplified. This instability, however, did not couple with the combustor acoustic modes and did not excite helical combustion instability.

In addition to decoupling the combustion process from the flow instability, the temperature became more uniform, and NO_x-forming high-temperature zones within vortices were eliminated while maintaining low CO production.

Acknowledgments

We gratefully acknowledge the assistance of Holger Ries for the phase-averaged flame pictures. The authors would also like to acknowledge the support of Wolfgang Weisenstein, ABB.

References

[1]Oster, D., and Wygnanski, I., "The Forced Mixing Layer Between Parallel Streams," *Journal of Fluid Mechanics*, Vol. 123, 1982, pp. 91–130.

[2]Ho, C., and Huerre, P., "Perturbed Free Shear Layers," *Annual Review of Fluid Mechanics*, Vol. 16, 1984, pp. 365–424.

[3]Crow, S., and Champagne, F., "Orderly Structure in Jet Turbulence," *Journal of Fluid Mechanics*, Vol. 48, No. 3, 1971, p. 567.

[4]Paschereit, C. O., Wygnanski, I., and Fiedler, H. E., "Experimental Investigation of Subharmonic Resonance in an Axisymmetric Jet," *Journal of Fluid Mechanics*, Vol. 283, 1995, pp. 365–407.

[5]Hasan, M. A. Z., "The Flow over a Backward Facing Step Under Controlled Perturbation: Laminar Separation," *Journal of Fluid Mechanics*, Vol. 238, 1992, pp. 73–96.

[6]Kailasanath, K., and Gutmark, E., "Combustion Instabilities," *Developments in Propulsion and Combustion*, edited by G. Roy, Taylor and Francis, Washington, DC, 1998, pp. 129–172.

[7]Schadow, K. C., and Gutmark, E., "Combustion Instability Related to Vortex Shedding in Dump Combustors and Their Passive Control," *Progress of Energy and Combustion Science*, Vol. 8, 1992, pp. 117–132.

[8]McManus, K. R., Poinsot, T., and Candel, S. M., "A Review of Active Control of Combustion Instabilities," *Progress of Energy and Combustion Science*, Vol. 19, 1993, pp. 1–29.

[9]Annaswamy, A. M., and Ghoniem, A. F., "Active Control in Combustion Systems," *IEEE Control Systems*, Vol. 15, No. 6, 1995, pp. 49–63.

[10]Rayleigh, J. W. S., "The Explanation of Certain Acoustic Phenomena," *Royal Institute Proceedings*, Vol. 8, 1878, pp. 536–542.

[11]Gutmark, E., Parr, T. P., Wilson, K. J., Hanson-Parr, D. M., and Schadow, K. C., "Use of Chemiluminescence and Neural Networks in Active Combustion Control," *Proceedings of the Combustion Institute*, Vol. 23, 1990, pp. 1101–1106.

[12]Schadow, K. C., Gutmark, E., and Wilson, K. J., "Active Combustion Control in a Coaxial Dump Combustor," *Combustion, Science and Technology*, Vol. 81, No. 4–6, 1992, pp. 285–300.

[13]Paschereit, C. O., Gutmark, E., and Weisenstein, W., "Structure and Control of Thermoacoustic Instabilities in a Gas-Turbine Combustor," *Combustion, Science and Technology*, Vol. 138, No. 1–6, 1998, pp. 213–232.

[14]Paschereit, C. O., Gutmark, E., and Weisenstein, W., "Coherent Structures in Swirling Flows and Their Role in Acoustic Combustion Control," *Physics of Fluids*, Vol. 11, No. 9, 1999, pp. 2667–2678.

[15]Paschereit, C. O., Gutmark, E., and Weisenstein, W., "Excitation of Thermoacoustic Instabilities by the Interaction of Acoustics and Unstable Swirling Flow," *AIAA Journal*, Vol. 38, No. 6, 2000, pp. 1025–1034.

[16]Paschereit, C. O., Gutmark, E., and Weisenstein, W., "Control of Thermoacoustic Instabilities and Emissions in an Industrial Type Gas-Turbine Combustor," *Proceedings of the Combustion Institute*, Vol. 27, 1998, pp. 1817–1824.

[17]Paschereit, C. O., Gutmark, E., and Weisenstein, W., "Suppression of Combustion Instabilities by Acoustic Control of Shear Layer Properties," *Advances in Turbulence*, edited by U. Frisch, Kluwer Academic, Norwell, MA, 1998, pp. 293–296.

[18]Paschereit, C. O., Gutmark, E., and Weisenstein, W., "Acoustic Control of Combustion Instabilities and Emissions in a Gas-Turbine Combustor," *Proceedings of the 1998 IEEE International Conference on Control Applications*, Italy, 1998.

[19]Cattolica, R. J., "OH Radical Non-Equilibrium in Methane-Air Flat Flames," *Combustion, Science and Technology*, Vol. 44, No. 1–3, 1982, pp. 43–50.

[20]Paschereit, C. O., Gutmark, E., and Weisenstein, W., "Control of Combustion Driven Oscillations by Equivalence Ratio Modulations," American Society of Mechanical Engineers, ASME 99-GT-118, June 1999.

[21]Pepperhoff, W., *Temperaturstrahlung*, Dietrich Steinkopff Verlag Gmbh and Co. KG, Berlin, 1956.

[22]Lieuwen, T., and Zinn, B. T., "The Role of Equivalence Ratio Oscillations in Driving Combustion Instabilities in Low NOX Gas Turbines," *Proceedings of the Combustion Institute*, Vol. 27, 1998, pp. 1809–1816.

[23]Gutmark, E., Parr, T. P., Hanson-Parr, D. M., and Schadow, K. C., "On the Role of Large and Small-Scale Structures in Combustion Control," *Combustion, Science and Technology*, Vol. 66, No. 1–3, 1989, pp. 107–126.

[24]Glassman, I., *Combustion*, Academic Press, San-Diego, CA, 1977, pp. 318–375.